

SCIENTIFIC REPORTS



OPEN

Optical properties of functionalized nanodiamonds

V. Pichot¹, O. Muller², A. Seve¹, A. Yvon², L. Merlat² & D. Spitzer¹

Detonation nanodiamonds exhibit strong nonlinear optical properties depending on their electronic properties. In the present paper, the nanodiamond functional groups are chemically modified to obtain nanodiamonds with primary amines on their surface. The optical properties of such nanodiamonds placed in water suspensions are studied and compared with the one of classical detonation nanodiamonds. Transmission, scattering and Z-scan experiments are performed for two different wavelengths (532 nm and 1064 nm). A lower threshold for optical limiting associated to more pronounced non-linear optical effects is detected at the wavelength of 1064 nm compared to the one at 532 nm. This effect may be due to a stronger nonlinear backscattering behavior at 1064 nm. Moreover, a striking result obtained from the Z-scan experiments reveals a completely different behavior of the functionalized nanodiamonds for both wavelengths. This result is discussed in regard to the electronic properties of the material and possible charge transfer.

With the nanomaterial advent, the behavior of nanoparticles when submitted to an electromagnetic solicitation has been intensively studied. Among nanoparticles which are of great interest in the optical field, carbonaceous nanoparticles have demonstrated extremely interesting properties in order to develop nonlinear optical systems^{1,2}. Moreover, previous studies showed that well controlled detonation nanodiamonds (DNDs) suspensions or functionalized DNDs could greatly improve the nonlinear properties of such material^{3,4}.

DND is a material of great interest due to its small size, the numerous functional groups present at its surface and its electronic properties. The variety of functional groups that can be found on the DND surface is depending on the purification or post purification treatments. In this manner, oxygenated, hydrogenated, chlorinated groups can be found on the DND surface^{5–10}.

In previous studies, Schmidlin *et al.* showed the presence of hydroxyl and carboxylic acid groups on DNDs purified under air treatment⁵. While carboxylic acids were mainly located on the most reactive parts of the particles most of the surface was covered with hydroxyl groups. The work of Shenderova *et al.* is in good agreement with these results¹¹. Research groups modified the DNDs surface functional groups into hydrogenated ones by using plasma or heat treatment under hydrogen flow in order to produce individual DND suspensions or to use them for functionalization or medical applications^{6,8,12}. Krüger *et al.* showed wide possibilities to functionalize the diamond with several functional groups and molecules¹⁰.

Varying the functional groups may change the electronic properties of the material and therefore change their optical properties¹³. Sasagawa *et al.* showed by using ultraviolet photon spectroscopy that the Fermi level of hydrogenated diamond is modified compared to the one of oxygenated nanodiamonds.

The goal of this study is to obtain nanoparticles with nonlinear properties to serve as optical filters to limit the effect of aggressive laser toward optronic systems (sensors, eyes...). DNDs can be used in suspension in appropriate solvent or in composites material such as polymers. For this purpose, functionalization can be necessary in order to maintain the DNDs in colloidal suspensions or for further integration in a solid matrix. Aminated DNDs seem very interesting for their possible interaction with hydroxyl groups of some polymers.

In this article, we describe the functionalization of DNDs with NH₂ groups on their surface by using a (S)-N-Boc-2,3-epoxypropylamine molecule. The optical properties of the modified diamonds are investigated in the green and near infrared region. The transmittance, scattering and z scan experiments are performed and reveal striking results for this complex.

¹NS3E "Nanomatériaux pour Systèmes Sous Sollicitations Extrêmes" UMR 3208 ISL/CNRS/UNISTRA, French-German Research Institute of Saint-Louis, 5 rue du général Cassagnou, 68301, Saint-Louis, France. ²Radiation Interaction with Matter Laboratory, French-German Research Institute of Saint-Louis, 5 rue du Général Cassagnou, 68301, Saint-Louis cedex, France. Correspondence and requests for materials should be addressed to V.P. (email: vincent.pichot@isl.eu)

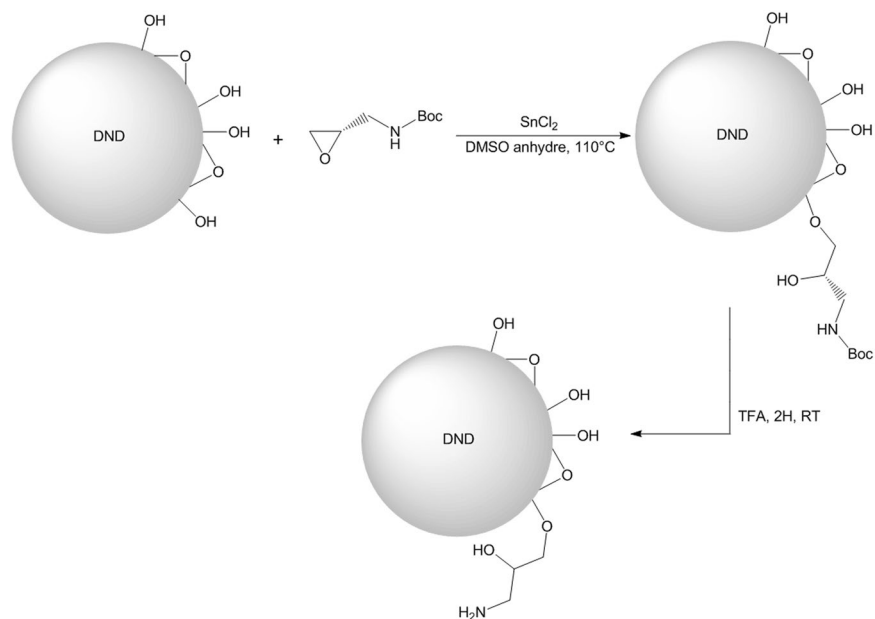


Figure 1. Reactional scheme of the DND functionalization. Functionalization of the nanodiamond surface with the (S)-N-Boc-2,3-epoxypropylamine molecule and deprotection of the amine group.

Results and Discussion

DND functionalization. The hydroxyl groups present at the DNDs surface were used in order to functionalize them. A DND particle with a diameter of 5 nm exhibits around 800 surface atoms. The quantity of (S)-N-Boc-2,3-epoxypropylamine used in the reaction was adjusted in order to graft around 100 of this molecule on the DND surface. The epoxy group of the (S)-N-Boc-2,3-epoxypropylamine molecule was used to form covalent bond with the OH groups¹⁴. The deprotection of the amine group was achieved to obtain the primary amine group. The reactional scheme is given in Fig. 1.

Different techniques (infrared and Raman spectroscopies, colorimetric tests) were used in order to prove the presence of the (S)-N-Boc-2,3-epoxypropylamine at the surface of the DND. These characterizations were unsuccessful probably due to the weak yield of this reaction.

A dye molecule (porphyrin) that can only be grafted on NH_2 groups was grafted on the functionalized DND in order to demonstrate the efficiency of the grafting with the (S)-N-Boc-2,3-epoxypropylamine molecule. This reaction was achieved by activation the carboxylic group of the (5-4-carboxyphenyl)-10,15,20-triphenyl-21,23-porphyrin with Hydroxybenzotriazole (HOBt) for the racemisation and Dicyclohexylcarbodiimide (DCC). This reaction was performed separately on both raw DNDs and DNDs grafted with deprotected (S)-N-Boc-2,3-epoxypropylamine (DND- NH_2). If one of these two samples (DND porphyrin and DND- NH_2 porphyrin) possess some primary amines groups, the porphyrin should be grafted at its surface after this reaction.

The samples were rinsed several time after the reaction with Dimethyl Sulfoxide (DMSO). DMSO is a very good solvent for this porphyrin. Finally, water was used to remove the remaining DMSO. The photoluminescence of the resulting DNDs was analysed by using the Raman spectrophotometer. The recorded spectra are given in the Fig. 2.

The spectra obtained from the samples containing DNDs show the signal from the DND at 552 nm and 561 nm corresponding to the diamond lattice vibrations band and to amorphous carbon or interstitial carbon atoms in the bulk of the crystallites respectively¹⁵. While the one of DND porphyrin is identical to the one of raw DND the spectrum of DND- NH_2 porphyrin reveals some additional photoluminescence bands at 650 and 713 nm. These bands are typical of the (5-4-carboxyphenyl)-10,15,20-triphenyl-21,23-porphyrin as shown from the spectrum of the porphyrin alone (blue curve). The blue shift of these photoluminescence bands can be attributed to interactions between the DNDs and the molecule due to the grafting of the porphyrin on the DNDs surface.

According to this result, we can clearly assume the successful grafting of the (S)-N-Boc-2,3-epoxypropylamine on the DND surface and the removal of the tert-Butyloxycarbonyl (Boc) protecting group function leading to the presence of NH_2 pending bond on the DND.

Nitrogen is present inside the DNDs crystals as defaults with yield of around 1–2 at.%. The variation of the nitrogen can vary by 1 at.% from one nanodiamond sample to another making quantitative studies such as XPS or elementary analyses very difficult to interpret. However, X-Ray Photoelectron Spectroscopy (XPS) measurements have been performed on DND and DND- NH_2 samples, the results are given in Table 1. No difference between the two samples could be noticed. Remaining Tin (Sn) coming from the SnCl_2 catalyst used in the reaction was detected in the DND- NH_2 sample. This means that even with several washing of the sample some Tin is still present in this sample.

The analysis of DND- NH_2 suspension performed by Dynamic Light Scattering (DLS) reveals a size distribution around 120 nm for the DND aggregates (Fig. 3). This size distribution is similar to the one obtained for the raw DND suspension and is classical for suspensions obtained from supernatant after 1 hour of ultrasound sollicitation and one day of sedimentation³. This means that the functionalization of the DNDs into DND- NH_2 did not lead to aggregation of the nanodiamonds as the concentration of the supernatant are identical.

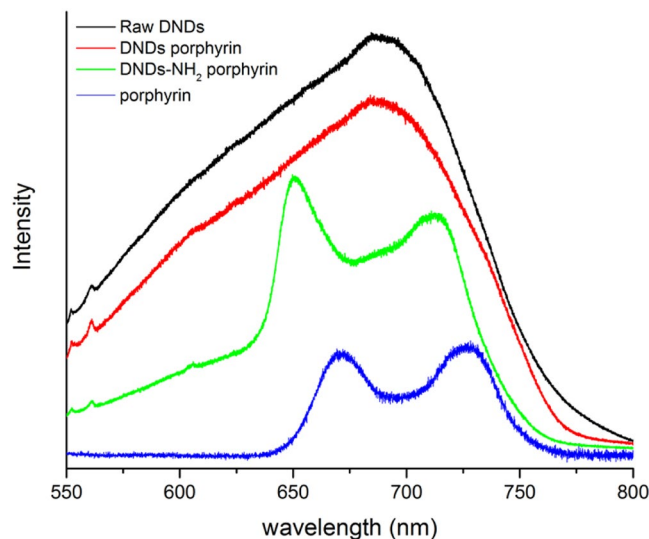


Figure 2. Photoluminescence spectra of the samples. Photoluminescence Raman Spectra obtained for DND (black), DND porphyrin (red), DND-NH₂ porphyrin (green) and porphyrin alone (blue). A 514 nm excitation wavelength was used.

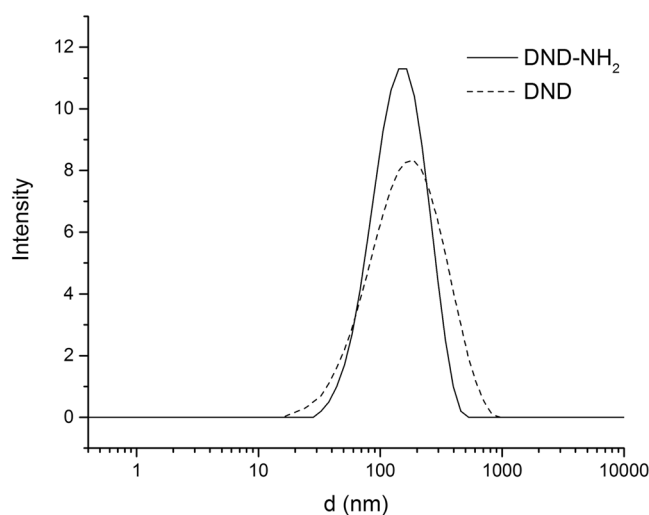


Figure 3. Size analyses of the DND samples. Dynamic light scattering of the raw DND and DND-NH₂.

Samples	signal	Position	At.%	St.Dev. %
DND	C 1s	285,00	87,46	0,28
	O 1s	531,00	10,75	0,14
	N 1s	399,00	1,80	0,28
DND-NH ₂	C 1s	285,00	85,79	0,31
	O 1s	530,50	11,63	0,16
	N 1s	398,50	1,83	0,30
	Sn 3d	485,00	0,74	0,05

Table 1. XPS quantitative measurements on DND and DND-NH₂ from C1s, O1s, N1s and Sn3d signals.

Nonlinear transmittance. Figure 4 shows the normalized nonlinear transmittances at both laser wavelengths (532 nm and 1064 nm) for the DND and DND-NH₂ suspensions in water. The input fluence was set to vary from 1 mJ/cm² to approximately 10⁵ J/cm². The observed behaviors for both nanomaterials are very similar. The energy or fluence thresholds for optical limiting assessed in such a way where the transmittance drops to 50% are the following at wavelengths of 532 nm and 1064 nm, respectively: 1200 J/cm² and 870 J/cm². At 532 nm,

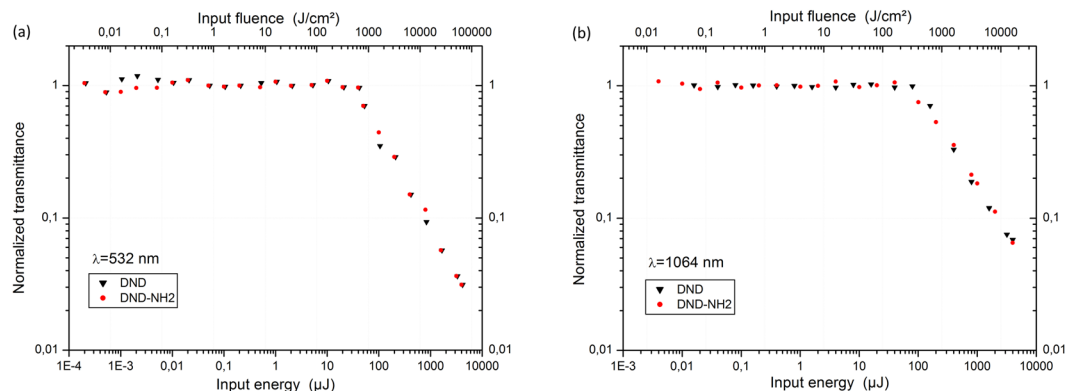


Figure 4. Non-linear transmittance experiments. Normalized transmittance as a function of the input energy and input fluence in a log-log scale. DND and DND-NH₂ suspensions in water at $\lambda = 532$ nm (a) and $\lambda = 1064$ nm (b) are represented.

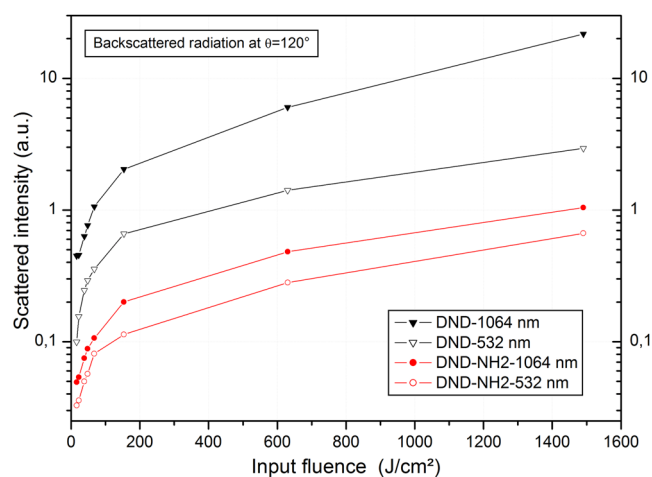


Figure 5. Non-linear scattering experiments. Semilog plot of the backscattered intensity ($\theta = 120$ degree) as a function of the incident fluence at $\lambda = 532$ nm (open symbols) and $\lambda = 1064$ nm (filled symbols) for the DND and DND-NH₂ suspensions.

a nonlinear attenuation corresponding to an optical density of 1.5 is achieved for both the DND and DND-NH₂ nanomaterials. At 1064 nm the trend remains approximately unchanged and an optical density of 1.2 is reached. In our experiments at 1064 nm (Fig. 4b) the transmittance drop begins at a slightly lower input fluence in comparison with the one at 532 nm (Fig. 4a). It is an interesting observation since the largest decrease in transmittance is obtained at 532 nm. This result is in contradiction with a previous study on metallic nanoparticles¹⁶. Accordingly, it is worth noting that the low threshold for optical limiting will be associated to more pronounced nonlinear optical effects at the wavelength of 1064 nm in the range $500 \text{ J}/\text{cm}^2$ to $1500 \text{ J}/\text{cm}^2$. Our postulate will be confirmed in a next section of this present work.

Nonlinear scattering. To better understand the reason that accounts for this threshold difference, nonlinear scattering measurements were conducted on DND and DND-NH₂ at both laser wavelengths. Generally speaking, after the laser has impacted the suspension, scattered waves are generated and propagate in all directions defined in a polar diagram¹⁷. It is obvious to say that only the backscattered waves contribute to the optical limiting phenomenon since these latter are rejected in a direction opposite to the sensor or the optronic device to be protected. In this way, we assessed the nonlinear backscattering properties of the DND and DND-NH₂ systems at an angle of 120 degree. The results are shown on Fig. 5 giving the scattered intensity as a function of the incident fluence in the range of interest.

It can be clearly seen that the scattered intensity is larger at a wavelength of 1064 nm for both nanomaterials especially for input fluencies above $600 \text{ J}/\text{cm}^2$. Figure 5 shows that the backscattered radiation is about a factor 10 more intense at 1064 nm compared to 532 nm in the case of the DND. However, this difference is less significant for the DND-NH₂. The strong nonlinear backscattering behavior at 1064 nm detected in the fluence range $[800-1500] \text{ J}/\text{cm}^2$ could explain a lower value for the onset of nonlinearities at 1064 nm as observed on the Fig. 4. Besides nonlinear scattering one can expect the occurrence of other optical nonlinearities like nonlinear absorption and nonlinear refraction¹⁸, or the electronic Kerr effect¹⁹. Our Z-scan measurements performed in a close

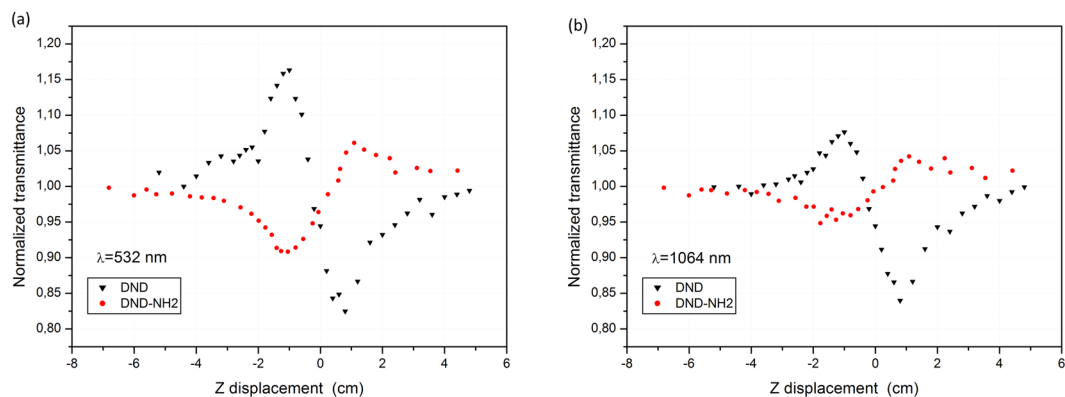


Figure 6. Z-scan experiments. Close Z-scan signatures of the DND and DND-NH₂ suspensions for an incident fluence of $F = 1000 \text{ J/cm}^2$. $\lambda = 532 \text{ nm}$ (a) and $\lambda = 1064 \text{ nm}$ (b). The curves reveal as well a self-defocusing effect (DND) and a self-focusing effect (DND-NH₂).

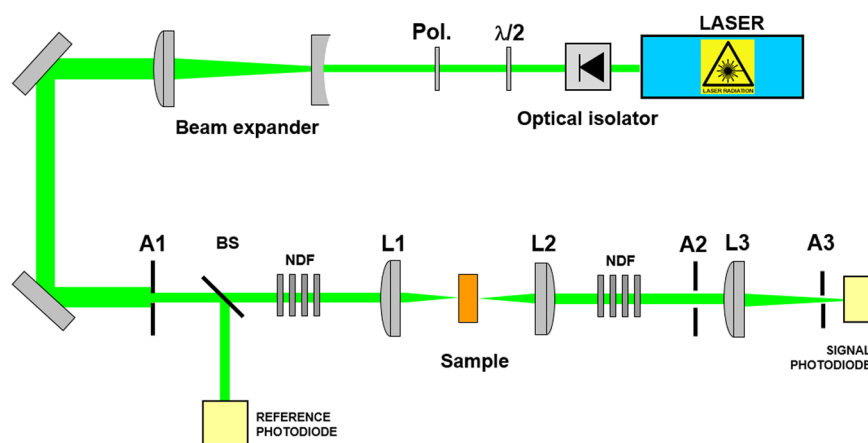


Figure 7. Optical experimental setup. Experimental setup used to study the optical limiting behavior of nonlinear nanomaterials samples. The denoted components are explained in the text.

aperture scheme will help to discriminate whether one of the aforementioned nonlinearity occurs in the DND and DND-NH₂ nanomaterials systems.

Z-scan experiments. The results are given in Fig. 6 reporting the normalized transmittance as a function of the Z sample displacement.

It is to be pointed out that symmetric Z-scan transmittance signatures are obtained at $\lambda = 532 \text{ nm}$ for both nanomaterials revealing that nonlinear absorption does not contribute to the observed phenomenon¹⁸ (Fig. 6a). Indeed, in the case of DND the peak to valley shape indicates a negative nonlinear refraction corresponding to a negative sign of the real part of the third order susceptibility²⁰ ($\text{Re}\chi^{(3)} > 0$). From a previous work of O. Muller *et al.*¹⁶, it is to be pointed out that such a result was expected since nanosecond duration laser pulses (this work, 4 ns) are mainly responsible for thermal lenses induced nonlinearities. Using the experimental results in Fig. 6 together with the analytical solution of the well-known Z-scan formalism detailed in¹⁶, the nonlinear refractive index, n_2 , of the DND was calculated to be $n_2 = -2.86 \cdot 10^{-16} \text{ cm}^2/\text{W}$ which denotes weak nonlinearities.

On the other hand, the valley to peak shape recorded in the case of the DND-NH₂ is somehow more surprising. Such a signature is subsequent to a self-focusing of the laser beam in the nonlinear sample, meaning, reversely to the former case, a positive sign of the real part of the third order susceptibility ($\text{Re}\chi^{(3)} > 0$). Generally speaking, such a behavior is observed when nonlinear materials are submitted to ultra-short laser pulses (hundreds of picoseconds and less) and is currently attributed to Kerr effects nonlinearities.

The DND-NH₂ sample contains NH₂ functional groups and remaining catalyst (Tin). Additional Z-scan experiments were performed on two complementary samples: raw DND mixed with SnCl₂ in water for one night at 110 °C and raw DND mixed with SnCl₂ in water for one night at 110 °C followed by a treatment with TFA the next day. For both samples, it was found the same peak-valley behavior like raw DNDs sample (not shown here). This means that the NH₂ functional groups is responsible of the valley to peak shape recorded in the case of the DND-NH₂.

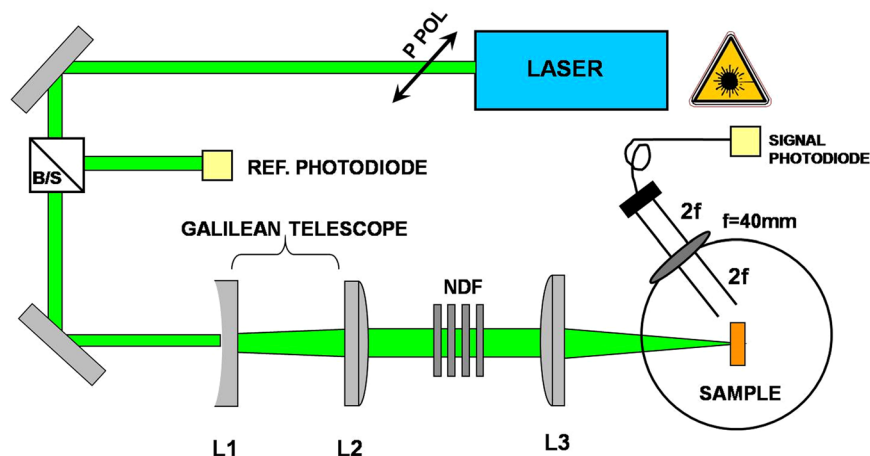


Figure 8. Experimental setup used to study the polar scattering properties. Details are in the text.

Assuming that intra and intermolecular charges transfer occur most likely in the DND-NH₂, the sign change of the nonlinear refractive index could be explained. However, such nonlinear phenomena take place on a pico-second timescale, which cannot be compared to the duration of the laser pulses of the present study. Accordingly, it might be possible that a tenfold occurrence of ultra short nonlinearities where molecular reorientational Kerr effect cumulates with enhanced charges transfer could be responsible for the observed valley to peak shape. Indeed, the NH₂ moiety could alternatively act as an electron donor (by conjugation) when the N atom, through its free electron pairs, participates to the resonance, or as a withdrawing group if the N atom cannot participate to the conjugation.

The same behavior is observed at $\lambda = 1064$ nm (Fig. 6b) and a value of $n_2 = -2.34 \cdot 10^{-16}$ cm²/W is deduced for the DND, similar to the one assessed at $\lambda = 532$ nm. However, the valley to peak shape shown for the DND-NH₂ is less pronounced in comparison to the case $\lambda = 532$ nm, thus a precise analytical calculation of the nonlinear refractive index could not be performed.

Conclusions

We have shown that chemically modified DNDs can exhibit a very different behavior to laser sollicitation compared to non-modified DNDs. While for both samples a more pronounced nonlinear backscattering behavior is observed at 1064 nm, the DND-NH₂ revealed a valley to peak shape in the Z-scan experiments, which can be attributed to Kerr nonlinearities effects. This very important result shows that it is possible to strongly influence the optical properties of the detonation nanodiamonds. Further studies are needed to better explain the origin of these phenomena especially by investigating the electronic properties of such materials.

Methods

Nanodiamonds were synthesized at the French German research institute of Saint-Louis (ISL) by detonation of high explosive mixtures (hexogen and trinitrotoluene) in a detonation chamber. After the explosion the detonation soot containing the DNDs is recovered by rinsing the detonation tank with deionized water. The DNDs purification is performed in two steps: an acid washing with a mixture of HCl/HNO₃ followed by an oxidation of the resulting soot at 380 °C.

The molecule used for the nanodiamond functionalization is (S)-N-Boc-2,3-epoxypropylamine (sigma aldrich 97%). Nanodiamonds (500 mg) were put together with (S)-N-Boc-2,3-epoxypropylamine (70 mg), SnCl₂ (70 mg) was added to serve as catalyst, the reaction was performed at 110 °C during 24 h in water (100 mL) under reflux with a magnetic stirring. After the reaction, the resulting product was rinsed several times with water and dimethylsuloxyde (DMSO sigma Aldrich, 99+%) over a 1 μm membrane filter (Millipore) to remove the (S)-N-Boc-2,3-epoxypropylamine excess. trifluoroacetate acid (14 mg, sigma Aldrich 99+%) and water (100 mL) were added at room temperature during 2 h under magnetic stirring to remove the tert-Butyloxycarbonyl protecting group (BOC group). The final product was then once again rinsed with water over a 1 μm membrane filter (Millipore) until obtaining a neutral pH.

A suspension of modified nanodiamonds was prepared in deionized water with a concentration of 1 g/L. After sedimentation of the biggest aggregates during 24 h, the stable supernatant phase was recovered and used for optical experiments.

A frequency doubled Nd:YAG laser system (Quantel) is used as the laser source, its output energy extents up to 400 mJ at 1064 nm and 160 mJ at 532 nm. The pulse repetition rate was fixed to 1 Hz and the pulse width is 4 ns. The experimental setup used to assess the nonlinear transmittance is shown in Fig. 7. The entrance aperture A1 was overfilled by the expanded beam so that a top-hat spatial irradiance distributed beam resulted. The nanomaterials samples were placed at the intermediate focal plane of a Keplerian telescope made of lens L1 and L2 with focal lengths of 60 mm and 100 mm, respectively. In front of the input lens L1 and behind the output lens L2, the apertures A1 and A2 (12 mm and 20 mm, respectively) were placed to achieve an optical system with a

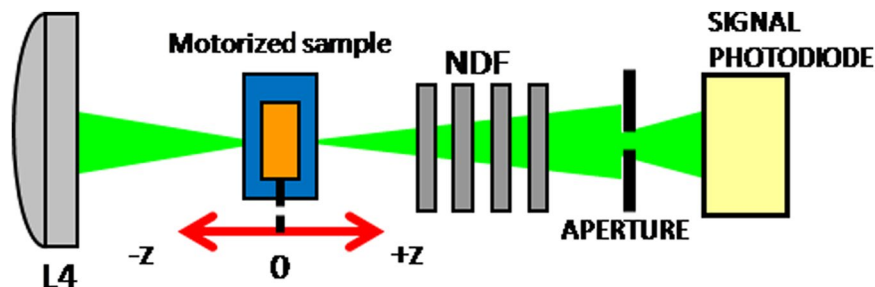


Figure 9. Z-scan experimental apparatus. The denoted components are explained in the text.

f -number of $f = 5$. With the help of a beam profiler (Cohu CCD camera), the focal diameter was estimated to be $4\ \mu\text{m}$ at $532\ \text{nm}$ and $8\ \mu\text{m}$ at $1064\ \text{nm}$. A part of the laser beam is splitted off by the beam splitter BS to monitor the incident energy, whereas the laser beam transmitted through the sample is further focused using the lens L3 (focal length $400\ \text{mm}$) to measure the signal energy. Additionally, the aperture A3 with an opening diameter of $600\ \mu\text{m}$ is positioned at the focal point of L3 toward the signal photodiode.

The setup used for the measurement of the polar nonlinear scattering is given on Fig. 8. Experimental details on the setup are reported elsewhere²¹. Shortly, the beam first expanded is focalized by the lens L3, $f_3 = 200\ \text{mm}$. The sample is set in the focal plane of L3 and the radius of the laser beam at the focus is $30\ \mu\text{m}$. The scattered signal is recorded on a photodiode mounted on a rotating stage used to collect the scattered light at an angle of 160 degree related to backscattering.

One part of the incident laser beam is taken from the main setup (Fig. 9) and directed toward the Z-scan setup in its close aperture scheme as shown in Fig. 2. The incident beam with a diameter of $7\ \text{mm}$ is focused into the sample area through the lens L4, $f_4 = 200\ \text{mm}$ in a $f/30$ focusing geometry⁴. The sample is placed on a motorized stage and is moved from $-z$ to $+z$. The emerging signal is collected on a photodiode before which we placed a $600\ \mu\text{m}$ aperture. The use of $1\ \text{mm}$ thin cuvettes follows the statement that the medium is to be considered as thin, i.e. a thickness smaller than the diffraction length of the focused beam¹⁶.

Raman spectra were recorded by using invia Renishaw spectrometer with a $514\ \text{nm}$ laser in photoluminescence mode including an edge filter and a grating of $1800\ \text{l/mm}$. Data were collected by a CCD camera.

Dynamic Light Scattering (DLS) was performed on a Malvern Instruments Zetasizer to measure the size of the nanodiamonds aggregates in suspension in water.

X-Ray Photoelectron Spectroscopy was achieved at the “Institut de Sciences des Matériaux de Mulhouse” (IS2M) with a VG SCIENTA “SES-2002” spectrometer, the samples were prepared on double sided adhesive carbon conductive tape. A monochromatic $\text{Al K}\alpha_{1,2}$ X-Ray source was used.

References

- Tutt, L. W. & Boggess, T. F. A review of optical limiting mechanisms and devices using Organics, Fullerenes, Semiconductors and other materials. *Progress in Quantum Electronics* **17**, 299–338 (1993).
- Mikheev, G. *et al.* Nonlinear scattering of light in nanodiamond hydrosol. *Technical Physics Letters* **36**, 358–361 (2010).
- Josset, S., Muller, O., Schmidlin, L., Pichot, V. & Spitzer, D. Nonlinear optical properties of detonation nanodiamond in the near infrared: Effects of concentration and size distribution. *Diam. Relat. Mater.* **32**, 66–71 (2013).
- Muller, O., Pichot, V., Merlat, L., Schmidlin, L. & Spitzer, D. Nonlinear optical behavior of porphyrinfunctionalized nanodiamonds: an efficient material for optical power limiting. *Appl. Opt.* **55**, 3801–3808 (2016).
- Schmidlin, L. *et al.* Identification, quantification and modification of detonation nanodiamond functional groups. *Diam. Relat. Mater.* **22**, 113–117 (2012).
- Williams, O. A. *et al.* Size-dependent reactivity of diamond nanoparticles. *ACS Nano* **4**, 4824–4830 (2010).
- Girard, H. A. *et al.* Hydrogenation of nanodiamonds using MPCVD: A new route toward organic functionalization. *Diam. Relat. Mater.* **19**, 1117–1123 (2010).
- Arnault, J. C. & Girard, H. A. Current Opinion in Solid State and Materials Science, <https://doi.org/10.1016/j.cossms.2016.06.007> (2016).
- Spitsyn, B. V. *et al.* Purification and functionalization of nanodiamond. in *Synthesis, Properties and Applications of Ultrananocrystalline Diamond* (Gruen, D. M., Shenderova, O. A. & Vul’ A. Ya. NATO Sciences series Springer, Dordrecht, 2005).
- Krueger, A. & Lang, D. Functionality is key: recent progress in the surface modification of nanodiamond. *Adv. Funct. Mater.* **22**, 890–906 (2012).
- Shenderova, O. *et al.* Surface chemistry and properties of ozone-purified detonation nanodiamonds. *J. Phys. Chem. C* **115**, 9827–9837 (2011).
- Stehlik, S. *et al.* Water interaction with hydrogenated and oxidized detonation nanodiamonds — microscopic and spectroscopic analyses. *Diam. Relat. Mater.* **63**, 97–102 (2016).
- Sasagawa, T. & Shen, Z. X. A route to tunable direct band-gap diamond devices: electronic structures of nanodiamond crystals. *J. Appl. Phys.* **104**, 073704 (2008).
- Liu, Y.-L., Chen, S.-C. & Liu, C.-S. Surface Grafting of Polyimide onto Silicon Surface: Preparation and Characterization. *J. Polym. Sci. PART A: Polym. Chem.* **45**, 4161–4167 (2007).
- Chapter 5 Raman and photoluminescence spectroscopy of detonation nanodiamonds 122–123 in *Detonation nanodiamonds Science and applications* (Vul’ A. Ya & Shenderova, O. A. Pan Stanford Publishing, 2014).
- Muller, O., Dengler, S., Ritt, G. & Eberle, B. Size and shape effects on the nonlinear optical behavior of silver nanoparticles for power limiters. *Appl. Opt.* **52**, 139–149 (2013).
- Nashold, K. M., Walter, D. P., Voss, J. M., Frysinger, G. S. & Sharpless, R. L. Comparing the scattering process in particle suspensions in liquids and gases for use as optical limiters. *Nonlinear Optics* **21**, 353–376 (1999).
- Samoc, M. *et al.* Nonlinear absorption and nonlinear refraction: maximizing the merit factors. Proc. of SPIE **8258**, Organic Photonic Materials and Devices XIV (2012).

19. Sheik-Bahae, M., Hagan, D. J. & Van Stryland, E. W. Dispersion and band-gap scaling of the electronic Kerr effect in solids associated with two-photon absorption. *Phys. Rev. Lett.* **65**, 96–99 (1990).
20. Ganeev, R. A., Rysnyansky, A. I., Kamalov, S. R., Kodirov, M. K. & Usmanov, T. Nonlinear susceptibilities, absorption coefficients and refractive indices of colloidal metals. *J. Phys. D: Appl. Phys.* **34**, 1602–1611 (2001).
21. Sheik-Bahae, M., Said, A. A., Wei, T. H., Hagan, D. J. & Van Stryland, E. W. Sensitive measurement of optical nonlinearities using a single beam. *IEEE J. Quantum Electron.* **26**, 760–769 (1990).

Acknowledgements

The Direction Général de l'Armenent (DGA) is acknowledged for their financial support.

Author Contributions

V.P. and O.M. directed the research. A.S. developed the idea of functionalization of the DND, V.P. achieved the functionalization and the Raman spectroscopy experiments. O.M. and A.Y. performed the optical and dynamic light scattering measurements. O.M. analyzed in details the optical experiments. V.P. and A.S. participated to the reflection about the characterization of the functionalized nanodiamonds. V.P. and O.M. wrote the paper, and all authors participated to the final version of the article by giving their advice and corrections.

Additional Information

Competing Interests: The authors declare that they have no competing interests.

Publisher's note: Springer Nature remains neutral with regard to jurisdictional claims in published maps and institutional affiliations.



Open Access This article is licensed under a Creative Commons Attribution 4.0 International License, which permits use, sharing, adaptation, distribution and reproduction in any medium or format, as long as you give appropriate credit to the original author(s) and the source, provide a link to the Creative Commons license, and indicate if changes were made. The images or other third party material in this article are included in the article's Creative Commons license, unless indicated otherwise in a credit line to the material. If material is not included in the article's Creative Commons license and your intended use is not permitted by statutory regulation or exceeds the permitted use, you will need to obtain permission directly from the copyright holder. To view a copy of this license, visit <http://creativecommons.org/licenses/by/4.0/>.

© The Author(s) 2017